NANO LETTERS

2005
Vol. 5, No. 6
1161−1164

Nanolithography Based on the Formation and Manipulation of Nanometer-Size Organic Liquid Menisci

Ramsés V. Martinez and Ricardo Garcia*

Instituto de Microelectrónica de Madrid, CSIC, Isaac Newton 8, 28760 Tres Cantos, Madrid, Spain

Received March 18, 2005; Revised Manuscript Received May 3, 2005

ABSTRACT

Nanometer-size menisci of organic liquids such as octane and 1-octene have been formed and used to confine chemical reactions. The application of a bias voltage between a conductive scanning probe tip separated a few nanometers from a silicon surface allows the field-induced formation of nanometer-size liquid menisci that can subsequently be used to fabricate nanometer-size structures. We report the fabrication of sub-10-nm nanostructures in 0.1 ms. Growth kinetics studies reveal that the nanostructure composition and its formation mechanism are organic-solvent-dependent. Both voltage polarities can be used to grow nanostructures, although the growth rate is significantly higher for positively biased samples. These experiments allow us to produce in the same sample two chemically different nanostructures that are easily addressed and positioned and have sub-10-nm features.

The past decade has seen the emergence of several scanning probe-based nanolithographies.[1−4] Among them, local oxidation or field-induced oxidation of semiconductor, metallic, and organic surfaces by atomic force microscopy (AFM) has established itself as a robust, reliable, and versatile lithographic method for the fabrication of nanometer-scale structures and devices.[5−11] In scanning probe-based oxidation, a water meniscus provides both the chemical species (oxyanions) and the spatial confinement for the anodic oxidation of a nanometer-size region of the sample surface.[12] The process is rather general because many different materials and/or surfaces have been patterned, such as semiconductors,[5,12,13] metals,[6−8,14] dielectrics,[9] polymers,[15,16] and self-assembled and dendrimer monolayers[17,18] among others. Furthermore, local oxidation can be scaled up by using stamps with multiple nanometer-size protrusions.[19−21]

We have also shown that nanostructures can also be fabricated by using polarizable organic solvents such as ethyl alcohol menisci.[22] In that case, the fabricated structures on a silicon surface were no longer oxides but showed the formation of silicon carbide and carbon sp^2 compounds.[23] Those experiments were mediated by the field-induced formation of nanometer-size menisci in a dynamic AFM interface. More recently, it was shown that operating the AFM in a liquid cell filled with *n*-octane gave rise to the formation of nanostructures that could be used as etch-resistant resists.[24] There the whole immersion of the tip in the liquid precluded the formation of nanometer-size meniscus. However, similar experiments performed in hexadecane gave rise to structures that showed chemical and kinetic behavior consistent with field-induced oxidation in air.[25] Those structures were easily etched in hydrofluoric acid (HF).

In this letter, we form and manipulate nanometer-size liquid bridges of nonpolar organic solvents such as octane and 1-octene with a dynamic force microscope. The liquid meniscus is used to confine the growth of nanometer-size structures as small as 8 nm in diameter. Nanostructures are fabricated at both polarities, although the resulting size is polarity-dependent. Chemical behavior and growth kinetic studies indicate that the composition of the fabricated structure is organic-solvent-dependent. The controlled formation of nanometer-size liquid menisci from nonpolar organic solvents reveals the general character of the AFM nanolithography based on the field-induced generation of chemical reactions because it applies to both polar and nonpolar fluids as well as vapor and condensed phases.

The experiments were performed with a dynamic atomic force microscope operated in the low-amplitude solution (noncontact)[26] and with additional circuits to apply voltage pulses.[12] The microscope was placed into an inner box with inlets for dry nitrogen and organic vapors. The inner box was enclosed in an outer box with an output to extract leaked organic vapors. First, the AFM chamber was purged of water vapor by flushing with dry N_2 for about 30 min. This reduced the relative humidity to below 2%. Then, the chamber was filled with either octane or 1-octane vapors (Sigma-Aldrich). Those vapors kept the relative humidity below 2%. Noncontact AFM nanolithography was performed with doped n^+-type silicon cantilevers (Nanosensors, Germany). The

* To whom correspondence should be addressed. E-mail: rgarcia@imm.cnm.csic.es.

10.1021/nl0505243 CCC: $30.25
Published on Web 05/13/2005

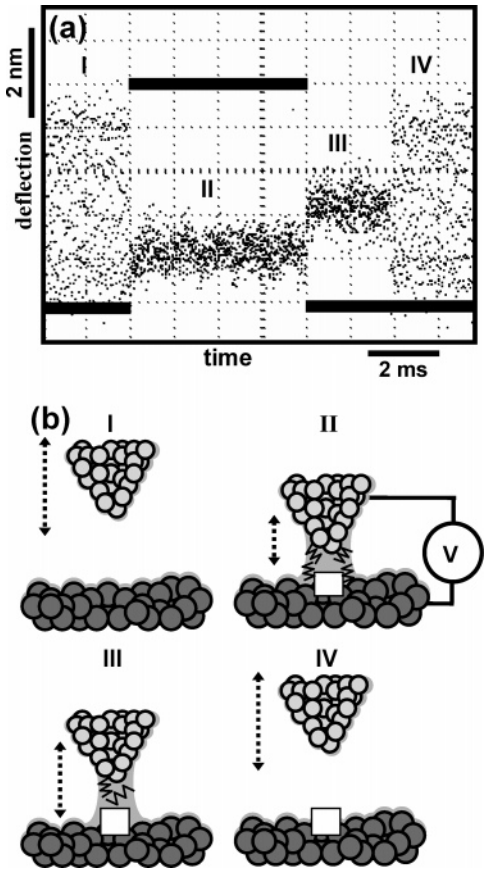

Figure 1. (a) Cantilever-tip oscillation (deflection) before (I), during (II), and after the application of a voltage pulse (III, IV) in an environment saturated with 1-octene vapor. Each dot represents the instantaneous AFM tip amplitude. Once the pulse is off, the octane meniscus holds the cantilever (III). Reestablishing the feedback breaks the meniscus (IV). Because the electrostatic force is higher than the capillary force, the cantilever moves its average position away from the surface when the pulse is off. The solid line represents the voltage pulse. (b) Interpretation of the deflection changes observed in part a and schematic of a single nanofabrication process. First, the tip is placed ~4 nm above the sample surface (I), and then a voltage is applied. The voltage deflects the cantilever, reduces the oscillation amplitude, and drives the formation of a liquid menisci (II). The nanolithographic process starts, and a nanometer-size feature is created (white box). After the voltage pulse is off, the attractive force of the liquid meniscus reduces the tip oscillation (III). Finally, the tip is retracted, and the original oscillation amplitude is recovered (IV).

force constant k and resonance frequency f_0 were about 35 N/m and 320 kHz, respectively. The cantilever was excited at its resonance frequency. The semiconductor samples were p-type Si(100) with a resistivity of 0.1−1.4 Ω cm. The numerical data presented in Figure 4 is the average of five nanofabrication experiments under the same conditions. The organic solvent menisci bridging tip and sample were field induced by applying an external voltage between the tip and sample. The reference electrode for the voltage is the tip, so positive (negative) polarity means that the sample is biased positively (negatively) with respect to the tip. The protocol is similar to the one previously applied to the field-induced formation of water and ethanol menisci.[22]

The formation of nanometer-size organic liquid bridges is monitored by following the instantaneous motion of the

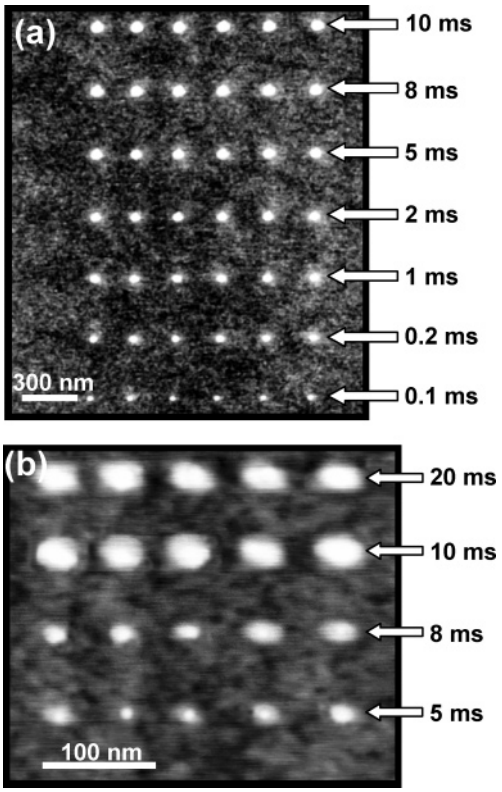

Figure 2. (a) Sequence of local modification experiments for different pulse times at a constant voltage (a) by forming octane menisci at 16.5 V and (b) by forming 1-octene menisci at 26 V.

AFM tip in an oscilloscope screen (Figure 1a). Before the application of a voltage pulse, the tip oscillates above the sample surface (I). The electrostatic interaction deflects the tip's equilibrium position and changes the AFM resonance frequency, which leads to a reduction of the oscillation amplitude (II). Once the pulse is off, the oscillation amplitude remains reduced because the capillary force of the organic liquid bridge holds the tip (III). Finally, the tip is retracted, which stretches and eventually breaks the bridge, and recovers its initial amplitude (IV). The nanofabrication process starts in II by increasing the pulse duration. A schematic of the process is depicted in Figure 1b.

In the presence of the liquid meniscus, the same or another voltage is used to initiate the nanolithographic process. The application of a single pulse generates a dot whose size depends on the voltage strength and pulse duration. Figure 2a shows several dots fabricated by the application of a series of 16.5 V pulses (sample positive) for different times in the presence of octane vapors. Each dot requires the formation of a nanometer-size meniscus. Dot lateral sizes are in the 20−70 nm range (full width). Figure 2b shows a similar experiment at 25 V with 1-octene menisci. Dot lateral sizes are in the 8−50 nm range (full width).

We have studied the dependence of dot formation with bias polarity (tip grounded). Nanostructures were formed at positive and negative polarities for both octane and 1-octene menisci, although they were significantly smaller at negative polarities (Figure 3). For the same pulse duration, positive polarities produced nanostructures of about 7 nm in octane

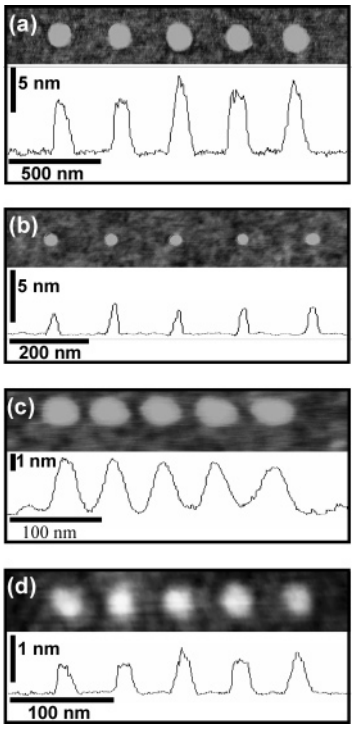

Figure 3. Dependence of the dot size with the voltage polarity. (a) Topographic AFM image and cross section of dots obtained in octane at positive polarity (21 V and 2.5 ms). (b) Topographic AFM image and cross section of dots obtained in octane at negative polarity (−21 V and 2.5 ms). (c) Topographic AFM image and cross section of dots obtained in 1-octene at positive polarity (26.5 V and 0.1 s). (d) Topographic AFM image and cross section of dots obtained in 1-octene at negative polarity (−26.5 V and 0.1 s). Positive polarities significantly favor the formation of the nanodots.

(i.e., about 5 times higher than at negative polarities (1.5 nm)). A similar ratio was obtained in 1-octene (3 vs 0.7 nm)

Cross-sectional images of the fabricated dots allow us to study the dependence of dot size on pulse duration. (Figure 4). The comparison among nanostructures obtained in octane and 1-octene menisci shows that the chemical nature of the liquid bridge has a determinant influence on the dot size. Dots obtained in octane grow faster and higher. The height seems to saturate at about 0.01 s. Actually, the application of longer pulses produces a dramatic modification of the sample surface with the uncontrollable formation of structures over several micrometer-squared regions. However, the growth kinetics of the dots formed in 1-octene environments is quite similar to the local oxidation kinetics of silicon surfaces in aqueous environments.[27] This is characterized by a high initial growth rate that decays rapidly and finally saturates. The main difference is that the local oxidation of the silicon surfaces starts at pulses one to two orders of magnitude longer. Heights are measured with respect to the baseline defined by the silicon surface, and widths are measured at the base of the nanostructure.

The semilogarithmic plot of height and width versus time of Figure 4 emphasizes three major results. First, it gives a protocol for obtaining dots of different sizes ranging from 8 to 70 nm, which would allow us to develop a reliable

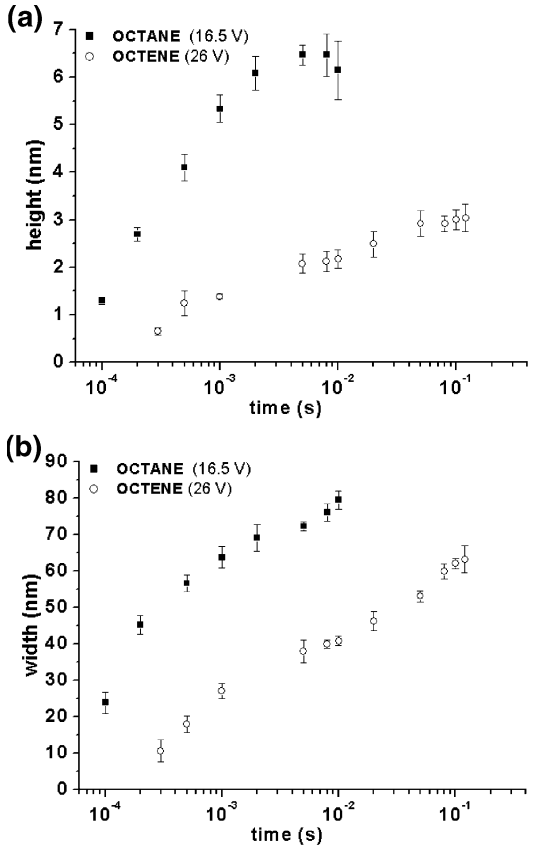

Figure 4. Semilogarithmic dot height (a) and width (b) dependence on pulse duration and liquid menisci composition. $V = 16.5$ and 26 V for octane and 1-octene, respectively.

nanolithographic process. Dots are the elemental features of AFM nanolithographies. Second, the kinetics is highly dependent on the chemical composition of the fluid. In octane, there is a rapid initial growth that abruptly self-terminates (before the process becomes uncontrollable), whereas in 1-octene the rapid initial growth rate slows down and self-terminates smoothly. Third, nanostructures could be easily formed with sub-0.1-ms pulses, which in turn would imply faster overall nanolithographic processes. The above kinetic results should also apply to experiments performed in liquid cells[24,25] because once the meniscus is formed the local tip−sample environment is identical.

To gain insight into the physical and/or chemical process behind the formation of nanostructures, we analyze the data plotted in Figure 4a with a power law parametrization that is commonly used in analyzing kinetic processes in local oxidation experiments,[28]

$$h = bt^{\gamma} \tag{1}$$

where h is the nanostructure height about the substrate baseline and t is the duration of the pulse. Parameters (b, γ) characterize the growth process, b depends on the voltage and liquid nature, and γ depends on the chemical nature of the fluid. For octane, we obtain (32 nm, 0.28), whereas for 1-octene we obtain (4.63 nm, 0.17). These values should be compared with the ones obtained in water and ethanol

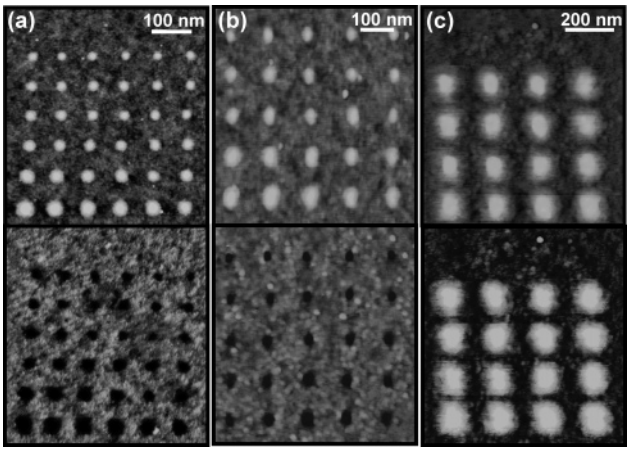

Figure 5. AFM topography images showing three arrays of dots patterned on Si(100) by using (a) water, (b) 1-octene, and (c) octane liquid menisci before (top pictures) and after exposure to HF (48%) vapors for 5 s (bottom pictures). Octane structures are HF-etch-resistant, whereas structures in water and 1-octene are readily etched.

environments (for similar voltages). Values of (9.3 nm, 0.32), and (3.48 nm, 0.12) have been reported for ethyl alcohol and water, respectively.[22] The kinetic parameters (b, γ) deduced for octane are the highest ones measured by scanning probe methods, whereas for 1-octene they are comparable to, albeit slightly higher than, those of water.

The high (b, γ) values obtained in octane allow us to conjecture a nonelectrochemical process where the formation of nanostructures is a two-step process—condensation of the octane molecules in the vicitnity of the AFM tip and then probably the polymerization of the hydrocarbon chains by the strong electrical field. We estimate that the electrical field in these experiments is about 10 V/nm. Those values are due to both the tip's sharpness and the tip−sample proximity. The above conclusion is consistent with the XPS analysis of the nanostructures obtained with ethanol menisci that revealed the presence of carbon sp^2 bonds that were attributed to either the formation of graphite or the polymerization of carbon chains.[23] It is also consistent with the experiments by Suez et al. where multiple depositions were achieved on the same spot.[24] However, 1-octene kinetic parameters are comparable to those of water. Those values indicate an electrochemical process similar to field-induced oxidation. Furthermore, 1-octene structures are readily etched by HF vapors as field-induced oxides, whereas octane nanostructures are etch-resistant in HF vapors and HF solutions alike (Figure 5). The samples for etching consisted of arrays of dots fabricated in water (air), 1-octene, and octane on the same piece of silicon. The nanostructures were simultaneously exposed to the same HF solution.

In short, we have formed and manipulated nanometer-size liquid menisci of organic liquids such as octane and 1-octene. These menisci have been used to confine chemical reactions that gave rise to the fabrication of nanometer-size structures. Two major results have been found: first, that the growth rate can be significantly modified by the composition of the organic solvent. We propose that in octane environments the field-induced formation of nanostructures requires the condensation and subsequent polymerization of carbon chains. The kinetics in 1-octene is very similar to field-induced oxidation processes, which suggests an electrochemical process. Second is the confirmation that scanning probe nanolithography based on the field-induced activation of chemical reactions is a general process that applies to both vapor and liquid phases, polar and nonpolar solvents, and contact and noncontact scanning probe microscopy interfaces. Furthermore, scanning probe nanolithography mediated by the formation and manipulation of liquid menisci allows us to produce in the same sample a variety of nanostructures of different chemical compositions that are easily addressed and positioned and have sub-10-nm features.

Acknowledgment. This work was supported by the MCyT (Spain) (MAT2003-02655) and the European Commission (NAIMO, IP NMP4-CT-2004-500355). We thank Marta Tello and Antonio García-Martín for useful suggestions.

References

(1) Quate, C. F. *Surf. Sci*. **1997**, *386*, 259.
(2) Cavallini, M; Biscarini, F; Leon, S.; Zerbetto, F.; Bottari, G.; Leigh, D. A. *Science* **2003**, *299*, 531.
(3) Ginger, D. S.; Zhang, H.; Mirkin, C. A. *Angew. Chem., Int. Ed*. **2004**, *43*, 30.
(4) Wouters, D.; Schubert, U. S. *Angew. Chem., Int. Ed*. **2004**, *43*, 2480.
(5) Dagata, J. A Schneir, J.; Harary, H. H.; Evans, C. J.; Postek, M. T.; Bennet, J. *Appl. Phys. Lett.* **1990**, *56*, 2001.
(6) Snow, E. S.; Campbell, P. M.; Buot, F. A.; Park, D.; Marrian, C. R. K.; Magno, R. *Appl. Phys. Lett*. **1998**, *72*, 3071.
(7) Matsumoto, K.; Gotoh, Y.; Maeda, T.; Dagata, J. A.; Harris, J. S. *Appl. Phys. Lett.* **2000**, *76*, 239.
(8) Bouchiat, V.; Faucher, M.; Thirion, C.; Wernsdorfer, W.; Fournier, T.; Pannetier, B. *Appl. Phys. Lett.* **2001**, *79*, 123.
(9) Chien, F. S.; Chou, Y.-C.; Chen, T. T.; Hsieh, W.-F.; Chao, T. S.; Gwo, S. *J. Appl. Phys.* **2001**, *89*, 2465.
(10) Garcia, R.; Tello, M.; Moulin, J. F.; Biscarini, F. *Nano Lett.* **2004**, *4*, 1115.
(11) Cooper, E. B.; Manalis, S. R.; Fang, H.; Dai, H.; Matsumoto, K.; Minne, S. C.; Hunt, T.; Quate, C. F. *Appl. Phys. Lett*. **1999**, *75*, 3566.
(12) Garcia, R.; Calleja, M.; Rohrer, H. *J. Appl. Phys.* **1999**, *86*, 1898.
(13) Xie, X. N.; Chung, H. J.; Xu, H.; Xu, X.; Sow, C. H.; Wee, A. T. S. *J. Am. Chem. Soc*. **2004**, *126*, 7665.
(14) Kuramochi, H.; Ando, K.; Tokizaki, T.; Yokoyama, H. *Appl. Phys. Lett*. **2004**, *84*, 4005.
(15) Lyuksyutov, S. F.; Paramonov, P. B.; Juhl, S.; Vaia, R. A. *Appl. Phys. Lett.* **2003**, *83*, 4405.
(16) Martin, C.; Rius, G.; Borrise, X.; Perez-Murano, F. *Nanotechnology*, in press, 2005.
(17) Maoz, R.; Frydman, E.; Cohen, S. R.; Sagiv, J. *Adv. Mater.* **2000**, *12*, 725.
(18) Rolandi, M.; Suez, I.; Dai, H.; Frechet, J. M. *Nano Lett.* **2004**, *4*, 889.
(19) Cavallini, M.; Mei, P.; Biscarini, F.; Garcia, R. *Appl. Phys. Lett.* **2003**, *83*, 5286.
(20) Hoeppener, S.; Maoz, R. Sagiv, J. *Nano Lett.* **2003**, *3*, 761.
(21) Farkas, N.; Comer, J. R.; Zhang, G.; Evans, E.A; Ramsier, R. D.; Wight, S.; Dagata, J. A. *Appl. Phys. Lett*. **2004**, *85*, 5691.
(22) Tello, M.; Garcia, R. *Appl. Phys. Lett.* **2003**, *83*, 2339.
(23) Tello, M.; Garcia, R.; Martín-Gago, J. A.; Martinez, N. F.; Martin-Gonzalez, M. S.; Aballe, L.; Baranov, A.; Gregoratti, L. *Adv. Mater*., in press, 2005.
(24) Suez, I.; Backer, S. A.; Frechet, J. M. J. *Nano Lett.* **2005**, *5*, 321.
(25) Reagan Kinser, C.; Schmitz M. J.; Hersam, M. C. *Nano Lett.* **2005**, *5*, 91.
(26) Garcia, R.; San Paulo, A. *Phys Rev. B* **1999**, *60*, 4961.
(27) Tello, M.; Garcia, R. *Appl. Phys. Lett*. **2001**, *79*, 424.
(28) Teuschler, T.; Mahr, K.; Miyazaki, S.; Hundhausen, M.; Ley, L. *Appl. Phys. Lett.* **1995**, *67*, 3144.

NL0505243